Interactions of nonlinear pulses in convection in binary fluids

James A. Glazier and Paul Kolodner
AT&T Bell Laboratories, Murray Hill, New Jersey 07974-2070
(Received 31 August 1990)

Several groups have recently reported a robust localized state of traveling waves in experiments on convection in binary fluid mixtures. These states resemble the "pulse" solutions of complex Ginzburg-Landau equations with subcritical bifurcations. We study the stability of these pulses experimentally by observing their interaction with high-frequency wave packets, which we inject into our annular convection cell by creating localized disturbances. We find that the spatial phase structure of pulses is central to their stability. An incident wave packet of sufficient amplitude can perturb the phase of the pulse so much that it loses stability and disappears, leading to a transition to a new state. Phase perturbations also determine the interactions between nearby pulses and the role of random fluctuations in the transition from a pulse state to a state in which slow traveling rolls fill the cell.

I. INTRODUCTION

One-dimensional convection in binary fluids has proved a useful model system for understanding the dynamics of nonlinear traveling waves. In fluid mixtures, besides the ordinary temperature-driven density gradient causing Rayleigh-Bénard convection (characterized by the Rayleigh number R), there is a Soret-effect-driven concentration diffusion described by the separation ratio Ψ.[1] For all accessible negative Ψ, the first instability of a thin fluid layer as R is increased above the threshold for the onset of convection R_c is to traveling waves. In an annular container, for weakly negative Ψ, at values of R just above onset, the typical behavior is dispersive chaos—the growth and sudden disappearance of spatially localized, slowly moving pulses composed of traveling waves, which appear in apparently random spatial and temporal patterns.[2] For more negative values of Ψ, the typical behavior is the formation of persistent, localized, nearly stationary patches of traveling waves in a quiescent background *(confined states)*.[3–5] For larger values of R, the fluid undergoes a transition to a spatially uniform cell-filling state either of stationary or traveling rolls.[6] In this paper, we focus on the stability of localized traveling-wave states for moderate values of Ψ near the onset of convection.

Niemela, Ahlers, and Cannell have recently described a confined state of traveling-wave convection in binary fluids (25% ethanol in water, corresponding to a separation ratio $\Psi=-0.08$) in both annular and rectangular experimental cells.[3] In both geometries, they observe one or more localized, stationary pulses of traveling waves with a well-defined pattern of phase velocities that vary across the pulse and a time-independent, stationary envelope. The mean traveling-wave frequency in the pulse is approximately one half of the Hopf frequency of the linear traveling waves at onset. They find that the pulses fit well the functional form derived by van Saarloos and Hohenberg from a fifth-order, complex Ginzburg-Landau equation.[7] These observations suggest that previously observed confined states in rectangular containers[8] are also pulse solutions, in the sense that their confinement is an intrinsic feature of the state and is unrelated to the presence of walls. Anderson and Behringer have also observed similar stationary or slowly drifting pulses in an annular geometry.[4] These pulses are stable, with little change in the shape for a range of $\epsilon\equiv(R-R_c)/R_c$ from -0.01 to 0.008 in an annular geometry and from -0.016 to 0.004 in a rectangular geometry. At the upper end of this range, both groups observe a transition to a state in which traveling waves completely fill the experimental cell.[3,4]

These experimental observations resemble in many respects theoretical predictions based on complex Ginzburg-Landau equations. Thual and Fauve first observed stationary pulses in numerical experiments on a quantic equation transformed to a frame comoving with its traveling waves:[9]

$$\frac{\partial A}{\partial t}=\epsilon A+(1+ic_1)\frac{\partial^2 A}{\partial x^2}+(1+ic_3)|A|^2A-(1-ic_5)|A|^2A\ , \tag{1}$$

where A is the amplitude envelope of the traveling waves, and c_1, c_3, and c_5 are real constants. Later work derived pulses as anlaytical solutions to this equation[10] and explained their existence using perturbation theory.[11] Recently, Van Saarloos and Hohenberg[7] showed that localized structures are generic for complex Ginzburg-Landau equations with subcritical bifurcations. Below $\epsilon=0$, the equation can produce either a single front separating a convecting region from a conducting region, or a "pulse," which resembles experimental localized states. There are several differences between the predictions of these theories and the observed behavior, however. First, in the model, pulses and fronts are stationary in the comoving frame; that is, they drift at the group velocity in the laboratory frame. Experimentally, pulses are stationary in the laboratory frame. The experimental pulses are stable for $\epsilon>0$, while the theory predicts a transition

to a cell uniformly filled with traveling waves at $\epsilon=0$. Another difficulty is that the theory is valid only for envelopes which vary slowly in space compared to the wavelength of the traveling waves, while the experimentally observed pulses are very narrow. Thus, the match between the analytical pulse shape and the experimental data appears to be fortuitous.

Deissler and Brand studied the effect of cubic nonlinear gradient terms (equivalent to fifth-order amplitude terms) on pulse propagation in a complex Ginzburg-Landau equation:[12]

$$\frac{\partial A}{\partial t}+v\frac{\partial A}{\partial x}=\epsilon A+(1+ic_1)\frac{\partial^2 A}{\partial x^2}+(1+ic_3)|A|^2A-(1-ic_5)|A|^4A-(\lambda_r+i\lambda_i)|A|^2\frac{\partial A}{\partial x}-(\mu_r+i\mu_i)A^2\frac{\partial A^*}{\partial x}, \quad (2)$$

where λ_r, λ_i, μ_r, and μ_i are real parameters that control the strength of the higher-order nonlinearities. The formation of stable pulses with well-defined envelopes occurs as in Eq. (1), but the velocity of the pulses is up to seven times lower, depending on the parameters. The pulses are also narrower and are asymmetric. However, in a single-field Ginzburg-Landau theory, it is only possible to obtain zero pulse velocity for a measure-zero set of parameters, while the pulse velocity is zero in the laboratory over a broad parameter range. This problem is the major obstacle to a theoretical understanding of experimental observations, though, recently, Barten *et al.* have found nearly stationary pulses in numerical integrations of the full Navier-Stokes equations.[13] In their calculations, a large-scale circulation of solute caused by the convective flow weakens the buoyant force at the leading edge of the front and enhances it at the trailing edge, slowing down the pulse to a small fraction of the traveling-wave group velocity.

While we do not understand the origin of the zero pulse velocity, we may still study the stability of pulses as a separate problem. Deissler and Brand have studied stability theoretically, examining the collisions between pulses using a pair of quintic equations with cubic cross-coupling terms.[12] In their study, they find four basic types of behavior: (1) a pair of oppositely propagating pulses can interact, attenuating each other but regrowing to their original saturated amplitude and shape; (2) the two pulses can annihilate each other; (3) one of the pulses can be annihilated while the other survives; and (4) both pulses can survive, but the envelope of one irreversibility alters to a lower-energy state with a different shape (a transition from a double-humped two-particle state to a single-humped one-particle state). While it would be interesting to try to reproduce all of these interactions experimentally, the zero velocity of experimental pulses makes it difficult to study pulse collisions.

We have performed an extensive series of measurements focusing on the stability of nonlinear pulses in binary-fluid convection. In particular, we have developed a technique to study the stability of pulses by striking them with propagating pulses of linear traveling waves *(wave packets)*. For small incident wave packets, we find that the stationary pulses behave as perfect absorbers with no reflected or transmitted traveling waves. For larger-amplitude wave packets, the phase of the packet resets the phase of the stationary pulse, and the incident wave packet causes the emission of a weak wave packet on the other side of the pulse. No reflection occurs, however, and the emitted wave amplitude is not a monotonic function of the incident amplitude. Still larger incident wave packets destroy the pulse a variable length of time after the collision. We have also examined interactions between nearly pairs of pulses. We find that they form unstable bound states which eventually result in the disappearance of one of the pulses. We find that the phase structure of the pulses is crucial in determining their interactions with wave packets and with each other. We have also investigated the role of fluctuations and convective instability in the transition to a cell filled with convective rolls.

II. EXPERIMENT

We have described our apparatus elsewhere.[2] The annular cell is formed by a plastic disc and ring clamped between a rhodium-plated, mirror-polished copper bottom plate and a saphire top plate. The cell dimensions are $d=0.301$ cm height $\times 1.73d$ radial width $\times 80.1d$ mean circumference. Cooling water circulates azimuthally over the top plate, and the bottom plate is heated electrically. The temperature difference applied across the fluid layer ΔT is typically 4.1 K and is regulated to ± 0.3 mK. We used a solution of 1.4 wt.% ethanol in water at a mean temperature of 27.1 °C, yielding a separation ratio $\Psi=-0.069$, a Prandtl number $P=6.62$, and a Lewis number $L=0.009$.[14] We fill the cell through two narrow fill tubes located at diametrically opposite locations, designated 90° and 270°. A metal bellows caps the end of the 270° tube, and a plastic plug the 90° tube. The metal bellows is mounted upright in the base of a vertical clear plastic tube ruled at regular intervals and containing a ball bearing. We inject controlled-amplitude wave packets by first raising the ball bearing to a measured height with a small magnet and then allowing it to fall on the bellows. The compression of the bellows forces a small amount of fluid into and out of the cell, producing a reproducible disturbance at the 270° fill tube which then decomposes into two oppositely propagating wave packets. For large-amplitude disturbances, a smaller pair of wave packets forms at the 90° fill tube as well.

We use standard shadowgraph techniques to observe the wave pattern.[15] A computer records the output from an annular array of 720 photodiodes at periodic time intervals to produce a space-time history of the pattern. The convection is always one dimensional, consisting of superpositions of waves which propagate azimuthally around the cell in opposite directions (here called "left going" and "right going"). We display the image intensity profile in real time. From the stored data, we can calculate the total traveling-wave amplitude for each time

step by spatial demodulation. We use hidden-line plots to display the time development of these spatial patterns. We can also determine the left-going and right-going wave amplitudes by complex demodulation.[15] Since complex demodulation is in essence a narrow-band, phase-sensitive filter, this technique also allows us to separate high-frequency linear waves from low-frequency nonlinear waves.

If we begin with a quiescent state below onset and raise the Rayleigh number to a small positive value of ϵ, the fluctuations present in the cell grow into a state containing both left-going and right-going traveling waves. However, because the fluctuations are very small, it takes a substantial amount of time for them to grow to significant amplitude. Before this happens, we can study the behavior of coherent traveling waves by injecting wave packets whose amplitude, though small, is much larger than background fluctuations. In each case, the disturbance initially forms a nearly Gaussian wave packet at the main fill tube at 270° and a smaller wave pocket at the second fill tube at 90°. The wave packets then split into left-going and right-going components (Fig. 1). Because ϵ is positive, they grow as they propagate, with a growth rate proportional to ϵ. Note that the space-integrated amplitude of the pulses in Fig. 1 increases, even though their peak height initially decreases.

We can separate the left-going and right-going wave packets using complex demodulation and fit the resulting envelopes to Gaussians to determine the positions of their centers, their amplitudes, and their widths. We find that the wave packets propagate with a dimensionless velocity [Fig. 2(a)] of $s = 1.38 \pm 0.05$, while linear stability calculations for traveling waves give a velocity of $s = 1.60$.[16] The origin of this difference is not understood, but we have observed similar discrepancies in group velocity in narrow cells over a wide range of Ψ.[6] For small wave packets, the integrated amplitude grows exponentially in time [Fig. 2(b)], and the width gradually increases [Fig. 2(c)], while the frequency stays constant.[17]

We did experiments of three basic types. Starting with a quiescent cell below the onset of convection, we increased the temperature difference to a positive value of ϵ and injected a controlled-amplitude disturbance. The result is the creation of one or more saturated nonlinear pulses. We also began with one or two saturated pulses and injected a controlled-amplitude wave packet to study the interactions between pulses and wave packets. Finally, we created multiple pulses and studied their interactions.

While we have made the cell as geometrically and thermally uniform as possible, some defects, which worsened since the previous experiments performed with this apparatus, had a minor effect on the results. First, as discussed below, the final location of pulses is not random, and this probably represents some sort of asymmetry. Second, measurements of the onset R_c reveal a slow downward drift at a fractional rate of approximately

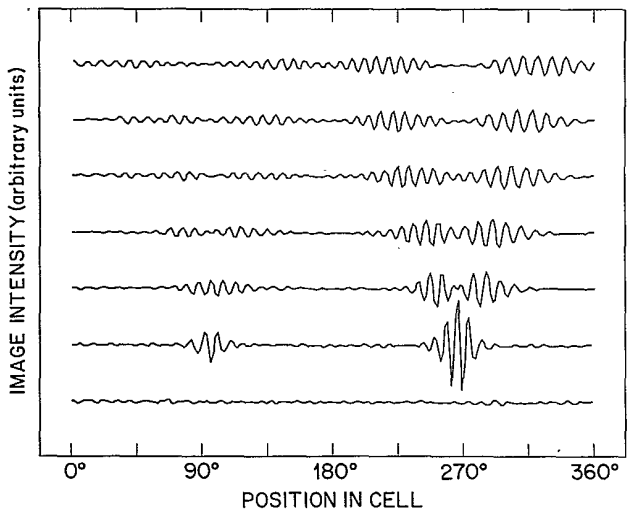

FIG. 1. Shadowgraph intensity as a function of position for seven successive 200-sec time steps (from bottom to top). Between the first and second time steps, we create a disturbance in an initially quiescent cell just above the onset of convection. The initial disturbances at the fill tubes split into left-going and right-going wave packets which propagate around the cell.

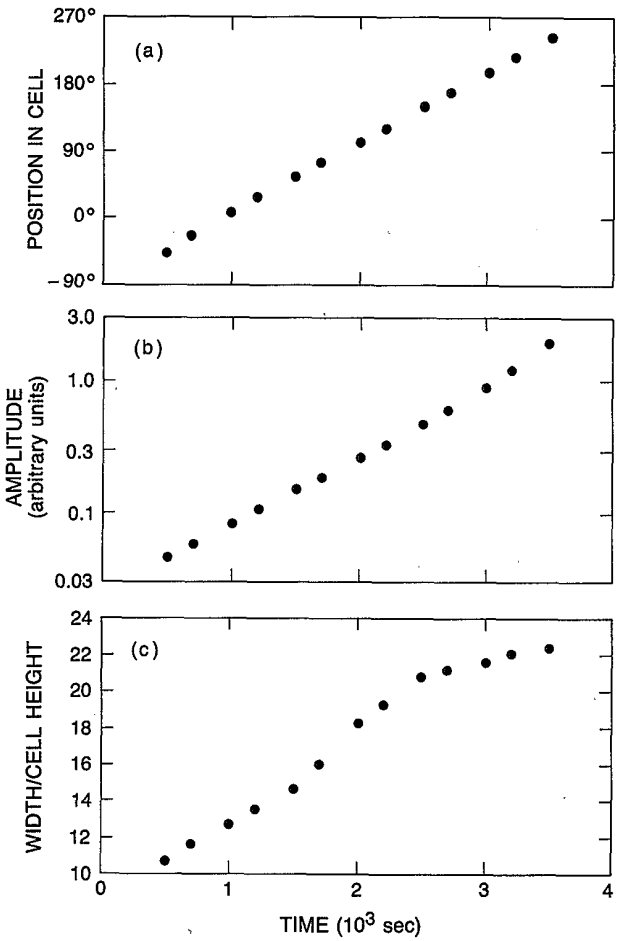

FIG. 2. (a) Position vs time of a typical linear wave packet ($\epsilon = 0.0054$) as in Fig. 1, showing its constant propagation velocity. (b) Wave amplitude (height times width) vs time for the wave packet, showing its exponential growth in amplitude. (c) Width of the wave packet (in units of cell height) vs time, showing its gradual spreading.

$(3-4)\times10^{-4}$ per day, possibly as a result of the loss of ethanol from the cell. This is not a serious problem, because the properties of the pulses are insensitive to the exact value of ϵ.[3] Also, the drift in Ψ during the experiment was negligible. We obtained the values of ϵ used in this paper by interpolating between measurements of R_c. We cross checked these results by measuring the growth rate of small wave packets; the linear growth rate γ is equal to ϵ times a measured proportionality constant.[1,16,18] We performed most of our experiments with $0.005<\epsilon<0.007$. To ensure that localized leaks do not cause any large-scale asymmetries, we took data only within two weeks of filling the cell. Since the original submission of this article, we have reproduced many of its results using an improved apparatus in which neither a drift in R_c nor a bias in the location of pulses was observed.

III. RESULTS

If we begin with a quiescent cell and inject a pair of disturbances, propagating wave packets circle the cell and grow in amplitude and width, passing through each other without interacting as long as their amplitudes remain small. As the wave packets grow, they begin to show nonlinear effects (Fig. 3). Though their integrated amplitude continues to increase, their width begins to decrease (at $t=2700$ sec). Slightly later ($t=3100$ sec), the wave packet stops completely and forms a stationary pulse of the type described in Ref. 3 [Figs. 4(a) and 4(b)]. Since the demodulation is tuned to the frequency of linear waves, the nonlinear frequency shift which accompanies the formation of the pulse causes the amplitude to drop after $t=3100$ sec. With the formation of a pulse, any remaining linear waves gradually disappear. De-

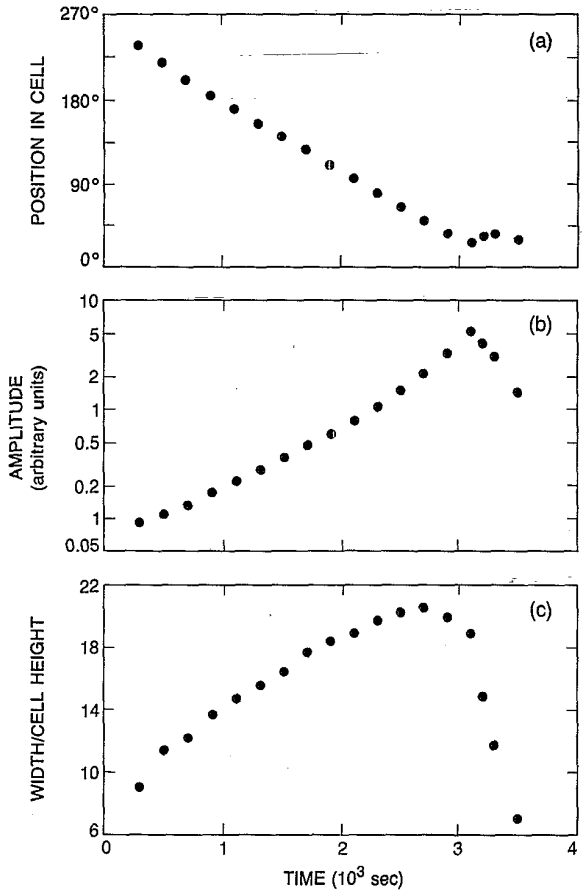

FIG. 3. (a) Position vs time for another growing wave packet at $\epsilon=0.0073$. (b) Amplitude of the wave packet vs time showing its exponential growth at early times. The apparent drop in amplitude starting at $t=3100$ sec is due to nonlinear effects which shift the oscillation frequency out of the bandwidth of the demodulation. (c) Width of the wave packet vs time. The width reaches a maximum at $t=2700$ sec, and a pulse forms at $t=3100$–3500 sec.

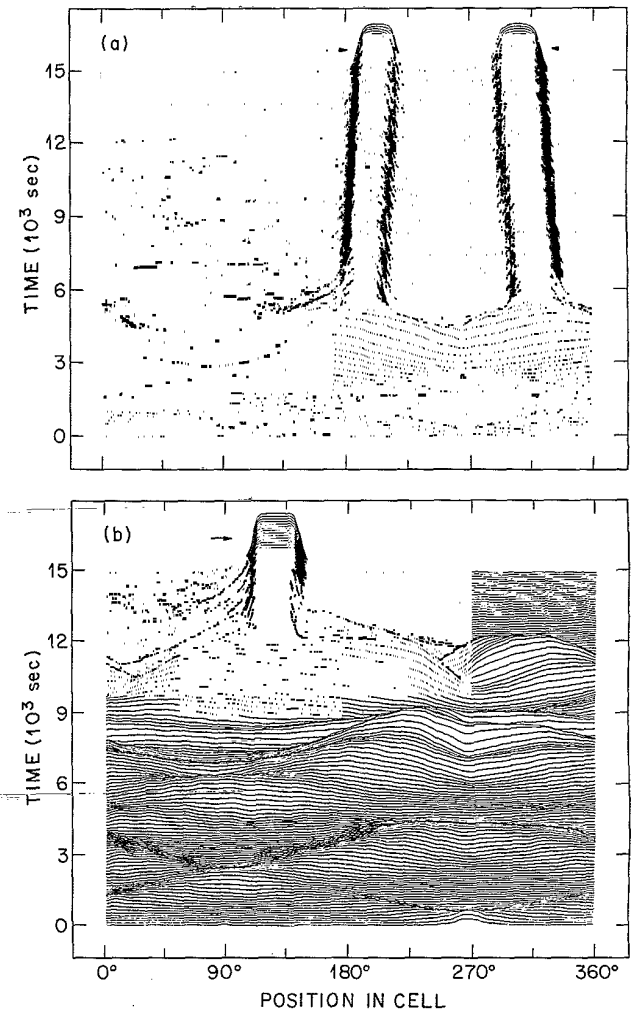

FIG. 4. (a) Hidden-line plot showing the growth of a weak disturbance injected into a quiescent cell at $\epsilon=0.0055$. The two resulting wave packets initially do not interact but grow up into two stationary pulses. (b) A disturbance injected into a quiescent cell closer to onset ($\epsilon=0.0015$) grows up into a single stationary pulse. In these hidden-line plots, each trace shows the total demodulated spatial amplitude profile at one instant in time, with time proceeding upwards. in order to suppress the contrast between the pulse and the weak wave packets, we plot the scaled hyperbolic tangent of the wave amplitude, which causes the pulses to appear flatter than they are.

pending on the amplitude of the injected disturbance and the rate of growth, the final pattern may be a pair of counterpropagating pulses [Fig. 4(a)] or a single pulse [Fig. 4(b)] with very small fluctuations in the rest of the cell. In all hidden-line plots, we plot $A_s \tanh(A/A_s)$, where A is the demodulated wave amplitude, and A_s is a saturation amplitude chosen to emphasize the low-amplitude waves. This clipping makes the pulses look more flat topped than they are. In these hidden-line plots, horizontal arrows indicate the direction of wave propagation under the stationary envelope of the pulse.

The pulses do not occur in random locations in the cell. Injected wave packets produce pulses located at well-defined positions symmetrically located with respect to the holes for the fill tubes. Frequently, left-going pulses are found between 300° and 330° and right-going pulses between 180° and 225°, as seen in Fig. 4(a). This symmetry is not surprising, since the fill tubes are the source of the waves which grow into pulses in experiments with injected disturbances. However, pulses which grow up from fluctuations also tend to drift to these positions, even though they seem to appear initially in random locations. The reason for these favored positions is unclear; possibly it results from a weak concentration gradient caused by leakage of ethanol from the fill tubes. The fixed locations of the pulses makes it easy to produce repeatable collisions and appears to have no other effect on the behavior of the system, so we have not attempted to eliminate it.

We now examine the interaction of a wave packet with a stationary pulse. In Fig. 5(a), we begin with two nearly stationary pulses; a left-going pulse on the right and a right-going pulse on the left. We then inject three disturbances of successively increasing amplitude. When the resulting wave packets reach the pulses (with respect to which their phase velocities are counterpropagating), they are completely absorbed. Any transmission or reflection would produce a growing wave packet, which

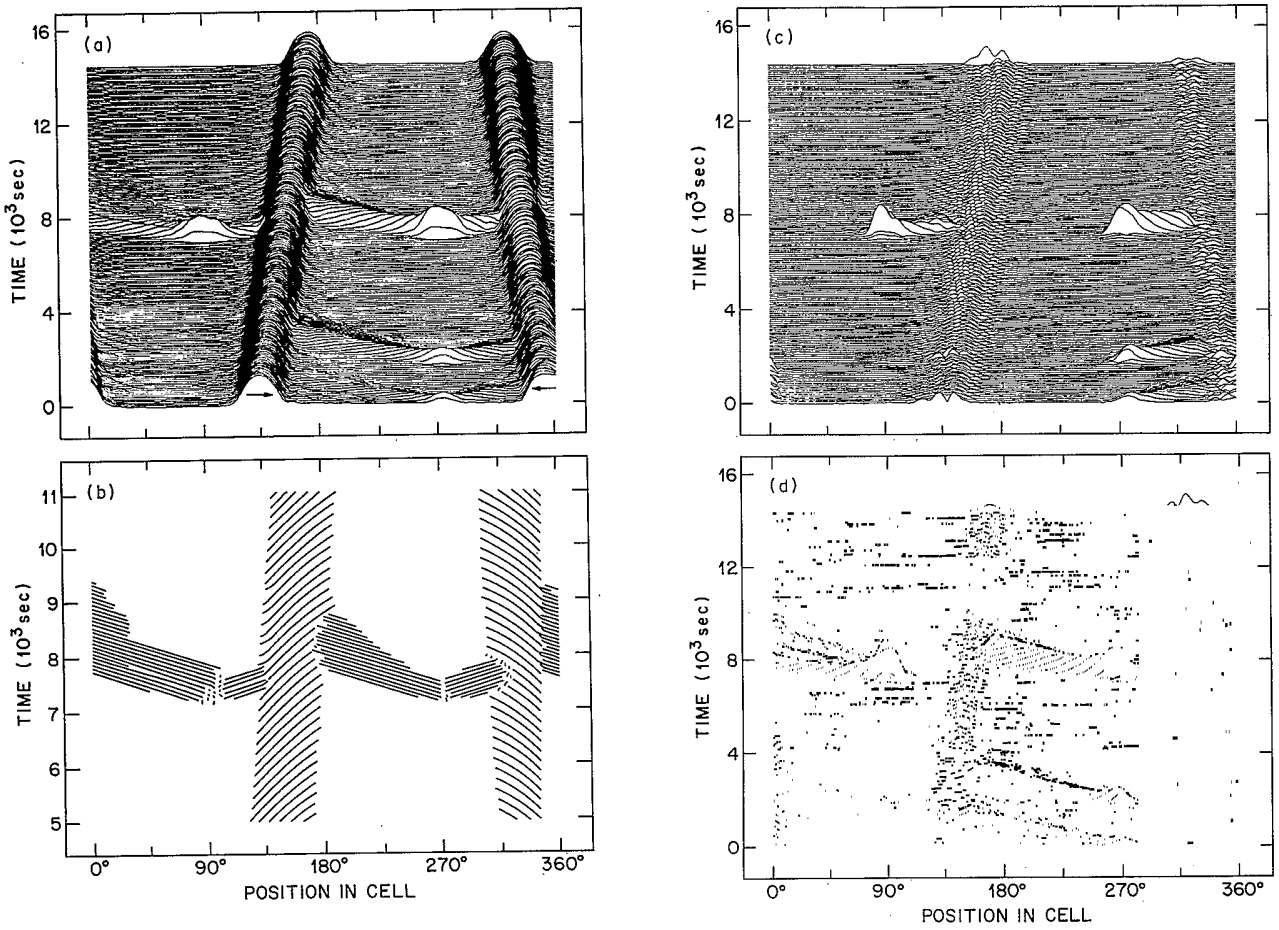

FIG. 5. (a) Hidden-line plot showing the interaction between slowly drifting pulses counterpropagating wave packets. The third disturbance is the largest we injected in any of our experiments. Note that, for the largest disturbance, the injection creates a smaller pair of wave packets at the opposite fill tube. (b) Phase plot of the interaction in (a) showing space-time contours of constant phase. Note that the phases of the counterpropagating wave packets penetrate the pulses but are advected out again. (c) and (d) Hidden-line plots of the same interaction using complex demodulation at the linear wave velocity to separate out (c) right-going waves and (d) left-going waves. Note that the absence of transmitted or reflected waves.

is not observed: to within the resolution of our measurements, there is no transmission or reflection of counterpropagating wave packets up to the highest possible injected amplitude.

We may follow the absorption process most easily by extracting the amplitudes of the left-going and right-going waves at the linear frequency [Figs. 5(c) and 5(d)]. The wave packets decay rapidly within the pulse. We also present a *phase plot* of the position of the individual wave crests versus time [Fig. 5(b)] to show the phase coherence of the pulses during the interaction. Even though the pulses completely absorb the incident wave packets, the higher-frequency wave packet's phase penetrates deeply into the pulse. However, because of the direction of wave propagation, the phase disturbance is quickly advected out of the pulse. As described in Ref. 3 and shown in Fig. 1 of Ref. 4, the phase velocities of the peaks grow as they propagate across the pulse, as shown by the curved constant-phase contours.

In Fig. 6(a), we show the interaction between a weak wave packet and a copropagating pulse. As in the case of a counterpropagating wave packet, the pulse appears to completely absorb the wave packet without reflection or transmission. The round-trip gain for the propagating wave packet in this case was 61. Thus, inspection of Fig. 6(a) shows that the transmitted wave is smaller than the incident wave packet by a factor α of at least 100. Employing complex demodulation and filtering to isolate possible transmitted and reflected wave packets gives a lower bound $\alpha \gtrsim 400$ for the attenuation of both transmitted and reflected amplitudes. Thus, in the presence of a pulse, the linear convective instability is suppressed above the onset measured with no pulse present by a fraction $\epsilon_c = s\tau_0\Gamma^{-1}\ln\alpha \gtrsim 0.013$, where s is the linear group velocity, τ_0 is the time scale of the growth of linear traveling waves, and $\Gamma = 80.1$ is the length of the system.[16,18] Probably, the absorption is total, and the pulse suppresses the traveling-wave instability completely.

Collisions between pulses and larger-amplitude wave packets are not so simple. We show a typical interaction

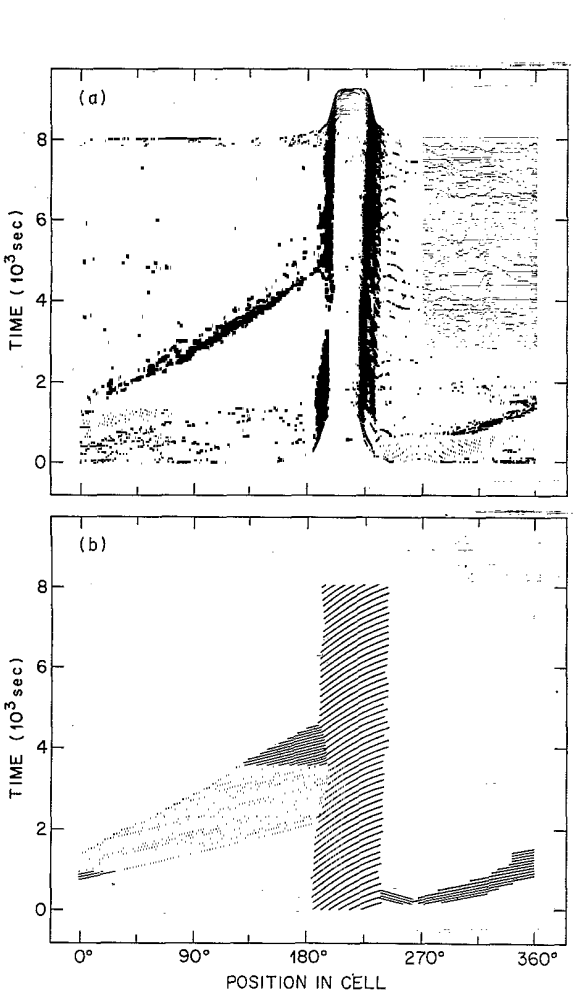

FIG. 6. (a) Hidden-line plot of the collision between a weak wave packet and a copropagating pulse. We do not understand the periodic rippling at the leading edge of the pulse. (b) Phase plot the collision shown in (a). The phase of the incident wave packets penetrates some way into the pulse but does not affect its phase.

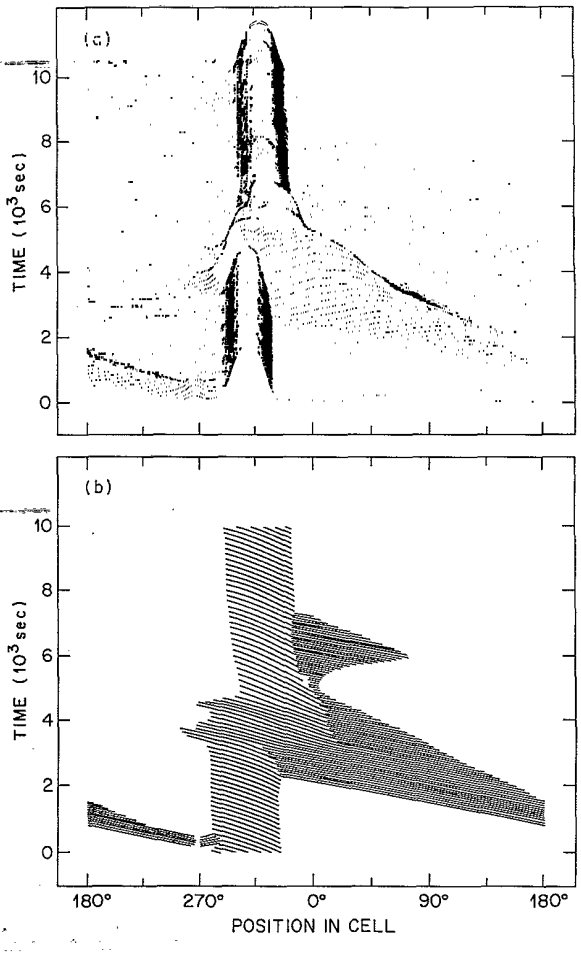

FIG. 7. (a) Hidden-line plot of the interaction between a strong wave packet and a copropagating pulse at $\epsilon = 0.0055$. (b) Phase plot of (a). Between $t = 3000$ and 4000 sec, the incident wave packet resets the phase of the pulse. The phase carries smoothly across the pulse for a few cycles. Note the extremely weak transmitted wave which collides with the pulse at $t = 6000$–8000 sec but does not reset its phase. We have shifted the horizontal axis by 180° for clarity.

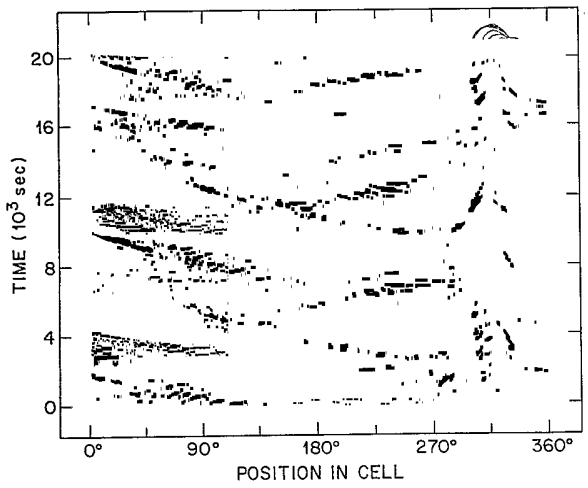

FIG. 8. Hidden-line plot showing that the transmitted amplitude is not a monotonic function of the incident amplitude ($\epsilon=0.0073$ throughout the run.) At $t=1500$ sec, a pair of copropagating pulses decays to produce a single left-going pulse. At $t=2000$ sec, we inject a disturbance, producing a strong left-going wave packet which then collides with the pulse at $t=5000$–6000 sec. Smaller copropagating wave packets produce larger transmitted packets. These grow into larger packets which, in turn, produce smaller transmitted waves.

between a wave packet and a copropagating pulse in Fig. 7(a). The phase plot [Fig. 7(b)] shows that the phase of the packet resets the phase of the pulse, the packet's phase carrying continuously across the pulse for a few cycles at the peak of the interaction. During the collision, the pulse broadens to a width intermediate between that of the undisturbed pulse and the incident packet. The wave packet, though attenuated, protrudes noticeably from the far side of the pulse. The incident wave packet eventually dies away, sometimes leaving the original pulse shifted slightly in the direction of the source of the wave packet.

Another important feature of the interaction is the emission of a narrow, small-amplitude wave packet on the other side of the pulse. In Fig. 7, the emitted wave packet is too weak to be seen initially, but, since the system is above onset, it grows up as it travels around the cell, becoming visible on the right side of the pulse, between $t=5000$ and 8000 sec. The emitted wave packet is initially narrower than the incident wave packet, so the pulse does not simply transmit the incident waves. Instead, the phase resetting of the pulse causes the emission of a wave packet. The same effect can also occur in other circumstances, as discussed below. Nevertheless, we can define a *transmission coefficient* η to be the ratio of the amplitudes of the incident wave packet and the transmitted wave. In no case is there any evidence for a reflected wave. The transmitted wave amplitude is not a monotonically increasing function of the incident amplitude. The transmitted wave of a very large incident wave packet is smaller than that of a slightly smaller incident wave packet. This can lead to the period-doubling behavior shown in Fig. 8, where a small incident packet generates a large transmitted packet, which in turn generates a small transmitted packet, etc.

The change between no transmitted wave and finite transmitted wave amplitude is a qualitative one. It is not that the transmitted waves of smaller incident wave packets are lost in the noise, but that the effective transmission coefficient increases from $\eta=0$ to $0.002<\eta<0.005$ for large incident wave packets, with η decreasing rapidly for still larger incident amplitudes until it returns to zero for the destructive regime described below. This "negative-resistance region" in the transmission coefficient plays a central role in the response of the system to random fluctuations, as discussed below.

As we further increase the incident-wave-packet amplitude, we find another qualitative change in the interac-

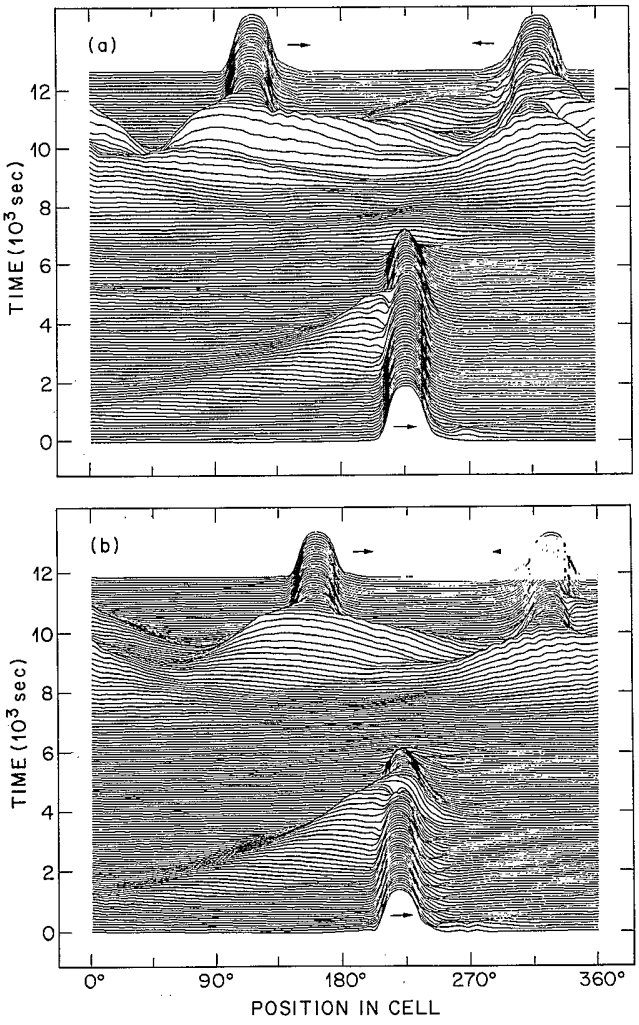

FIG. 9. (a) Hidden-line plot showing the long survival of a pulse after collision with a weak wave packet at $\epsilon=0.0058$. The disappearing pulse emits a pair of wave packets which then grow up into a pair of counterpropagating pulses symmetrically located with respect to the original pulse. (b) Hidden-line plot showing the shorter survival after collision with a stronger wave packet at $\epsilon=0.0053$. Again, the disappearing pulse emits wave packets which grow into almost symmetrical counterpropagating pulses.

tion. The incident wave packet annihilates the pulse. For very large incident wave packets, the annihilation may be immediate. For weaker wave packets, the pulse may take a considerable time to decay [Fig. 9(a)], the time decreasing with increasing strength of the incident pulse [Fig. 9(b)]. Even if the wave packet is not strong enough to destroy the pulse, the transmitted wave it generates can grow enough when it circles the cell to annihilation the pulse on a later collision [Fig. 10(a)]. While the shape of the pulse does not change, just after the collision its amplitude decreases slightly, and its phase is so strongly reset by the incident wave packet [Fig. 10(b)] that it loses stability and abruptly disappears. The wave packet which actually destroys the pulse causes no detectable transmitted wave in any of our data. Rather, the disappearance of the pulse generates counterpropagating wave packets which can grow up into a state of pulses [Figs. 9 and 10(a)] or a cell-filling state (Fig. 11).

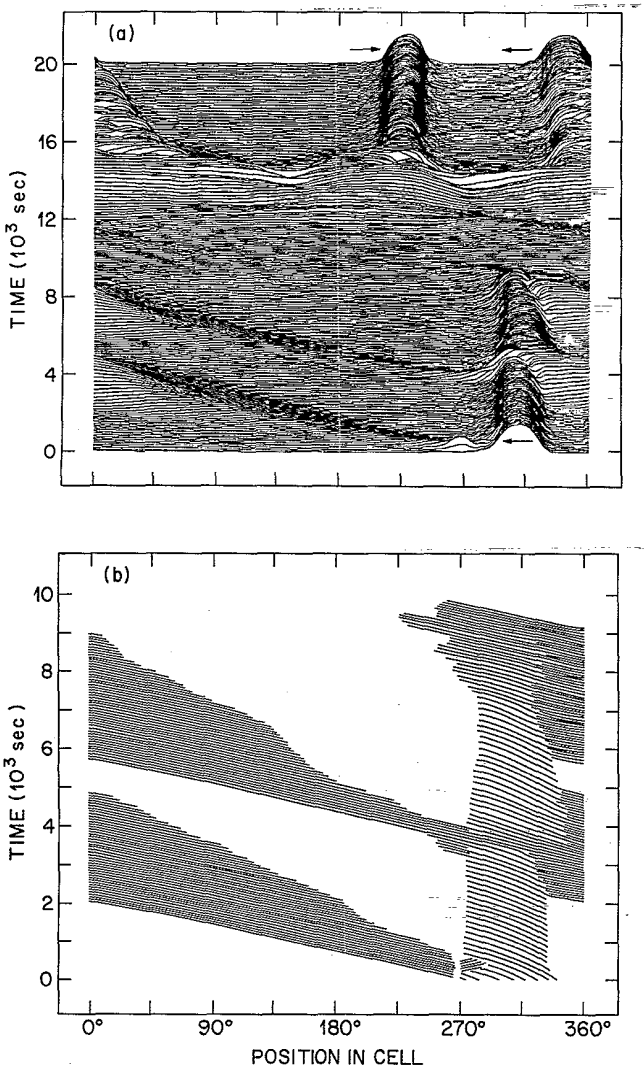

FIG. 10. (a) Hidden-line plot showing the annihilation of a pulse by a wave packet growing up from a transmitted wave at $\epsilon=0.0053$. The initial wave packet creates a transmitted wave but does not destroy the pulse itself. The transmitted wave then grows up to sufficiently large amplitude to destroy the pulse on the next collision. (b) Phase plot of the interaction in (a). The transmitted wave packet resets the phase of the pulse for many cycles, causing the pulse to dissolve into weak linear waves.

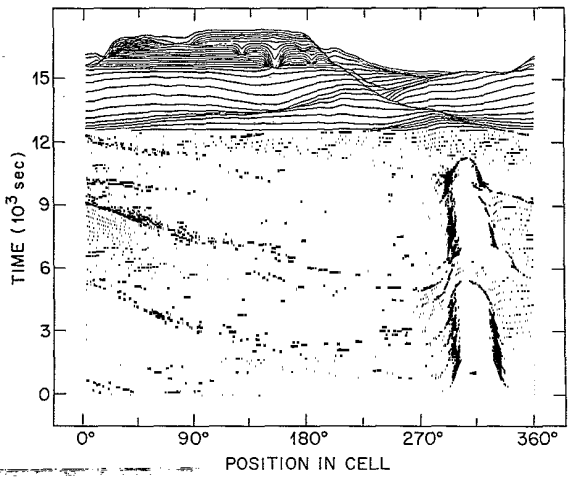

FIG. 11. Hidden-line plot showing the creation of a cell-filling state at $\epsilon=0.0061$ from a disappearing pulse. A weak, left-going wave packet collides with the pulse between $t=3000$ and 4000 sec. The transmitted wave then grows into a wave packet which destroys the pulse at $t=10000$ sec. The linear waves emitted by the decaying pulse and background fluctuations then grow up into a cell-filling state.

So far we have described the effect of injected wave packets on pulses. However, coherent propagating disturbances which arise from random fluctuations cause similar effects. These fluctuations determine the stability of stationary pulses. We show an example in Fig. 12, where random fluctuations cause a transition from a pulse to a cell-filling state at $\epsilon=0.0075$. In this system,

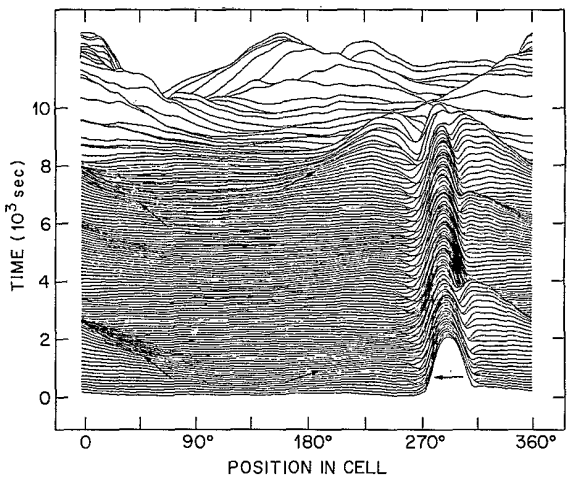

FIG. 12. Hidden-line plot showing the destruction of a pulse by spontaneous fluctuations at $\epsilon=0.0075$. In the first 8000 sec left-going and right-going disturbances (indicated by arrows) propagate in the cell. The fluctuations grow fast enough to destroy the pulse at $t=9000$ sec, creating a new state consisting of slow traveling waves which fill the cell.

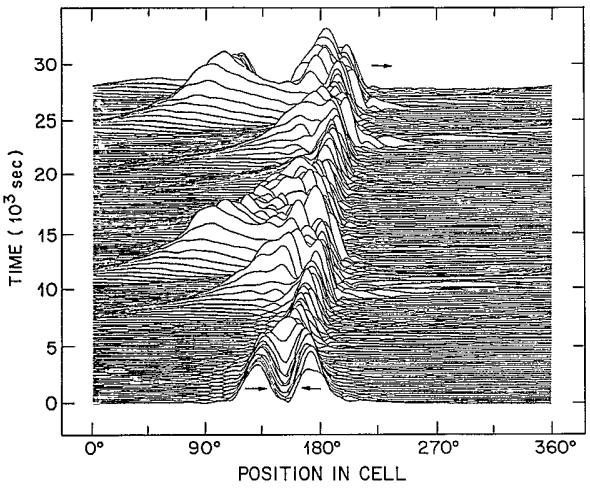

FIG. 13. Hidden-line plot showing the interaction between a pulse and background fluctuations at $\epsilon=0.0071$. The initial counterpropagating pair of pulses decay into a single right-going pulse (as in Fig. 15 below). The surviving pulse then interacts with trailing wave packets arising from fluctuations. Note the absence of left-going wave packets.

random fluctuations are always present above onset.[19] Because of the negative-resistance region in the transmission coefficient, these fluctuations tend to evolve into coherent wave packets (marked by arrows in Fig. 12). As noted previously, pulses absorb counterpropagating wave packets, while copropagating wave packets produce transmitted waves. These transmitted waves can build up enough amplitude, via a period-doubling sequence similar to the one in Fig. 8, to destroy the pulse, and thus lead to a cell-filling transition.

We believe that pulse destruction by coherent, fluctuation-driven wave packets imposes the fundamental limit on pulse stability. If so, the condition that such spontaneous fluctuations experience enough gain over the length of the system that their amplitude on collision with a pulse is sufficient to destroy it determines the threshold for the cell-filling transition ϵ_f. We can therefore estimate ϵ_f. The wave-packet amplitude required to destroy a pulse is three–eight times smaller than the amplitude of the full-cell state, which exhibits a spatial temperature modulation of amplitude 0.08 K ±50%.[18] Just below onset, the level of fluctuations is approximately 0.07–0.2 mK.[20] Thus, the system must be sufficiently above onset to produce a round trip gain $\gamma=40$–400 for fluctuations to cause the cell-filling transition. This gain occurs for $\epsilon_f=s\tau_0\Gamma^{-1}\ln\gamma\sim0.008$–$0.012$, which is near the observed threshold. We agree with Ref. 3 that the absolute traveling-wave instability, occurring at $\epsilon_a\sim0.06$, plays no role in the cell-filling transition.

Figure 13 illustrates another effect of fluctuation-driven wave packets. This run began with a pair of nearby counterpropagating pulses which decayed into a single pulse of right-going waves (we describe this pulse-pulse interaction below). Next, spontaneously generated,

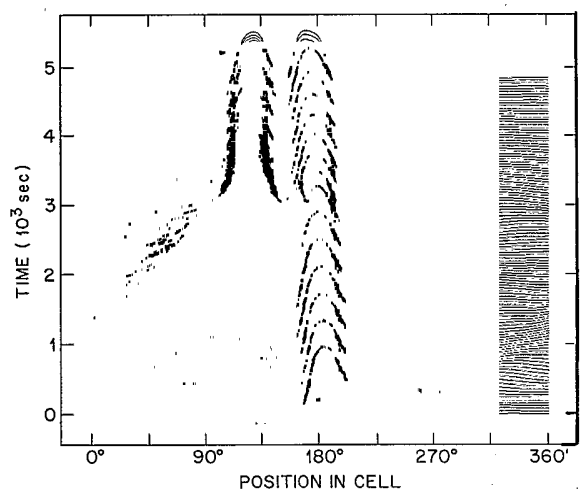

FIG. 14. Hidden-line plot showing the growth of an injected right-going wave packet into a right-going pulse at $\epsilon=0.0070$. The new pulse and the existing left-going pulse form a bound pair.

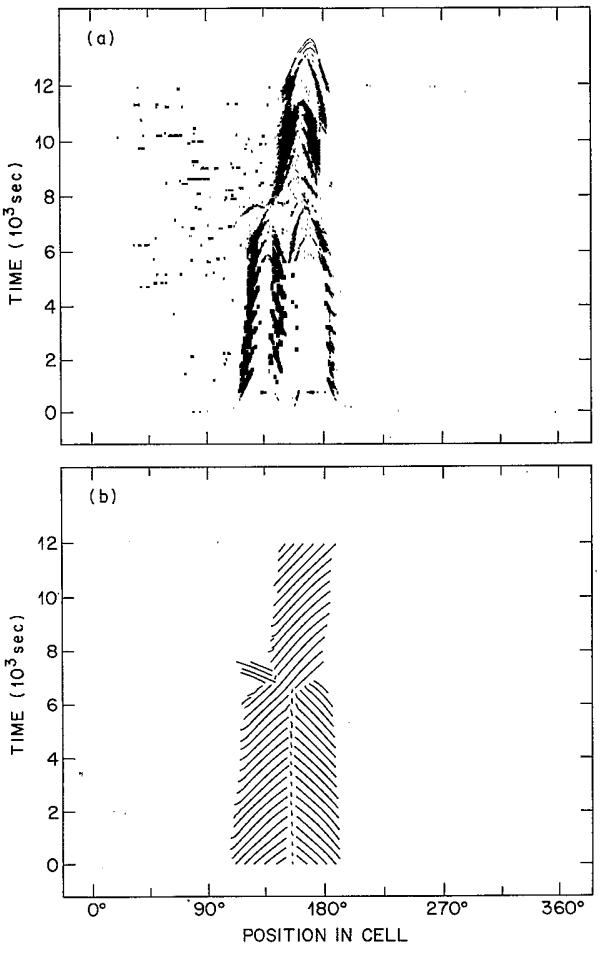

FIG. 15. Interaction between the counterpropagating pulses formed in Fig. 14. (a) Hidden-line plot showing the interaction of the pulses and the destruction of the right pulse. (b) Phase plot showing the phase singularity at the boundary between the pulses, the phase coherence of the final pulse with the left pulse, and the phase of the emitted left-going wave packet resulting from the interaction.

right-going wave packets appeared intermittently behind the pulse. Finally, these trailing wave packets produced a new stationary pulse (which is beginning to form at the top of Fig. 13, at location 110°). The processes revealed by our injected-disturbance experiments explain this behavior. There are no left-going (counterpropagating) waves because the pulse absorbs them completely, giving this space-time plot an asymmetric appearance. The state remained stable for a long time because of the "negative-resistance region" in the transmission coefficient η. If the pulse simply transmitted incident wave packets with a transmission coefficient that did not decrease above some amplitude, the cell would fill with rolls when the net round-trip gain exceeded the transmission loss. The nonmonotonic transmission coefficient saturates the wave-packet amplitude and gives the output leading edge of the pulse the appearance of a cliff bordering a plane. Finally, the trailing wave packets have a

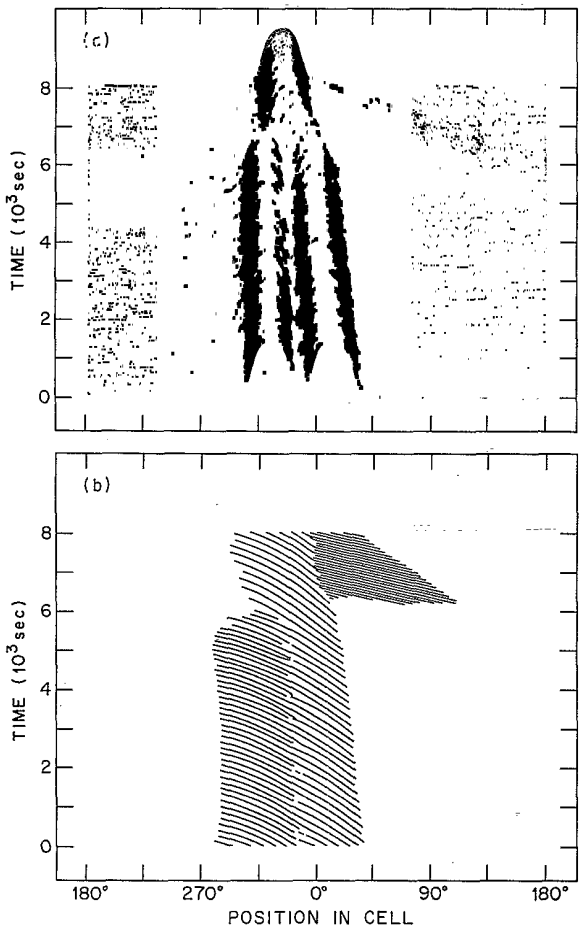

FIG. 16. Interaction between two copropagating pulses at $\epsilon=0.0078$. (a) Hidden-line plot showing the interaction between the pulses and the destruction of the leading (left) pulse. (b) Phase plot showing the phase dislocations caused by the phase-velocity mismatch between the leading pulse and the trailing pulse. Note the emitted wave packet, which is too small to see at first, but which becomes visible around $t=6000$ sec, after it has nearly circled the cell. We have shifted the horizontal axis by 180° for clarity.

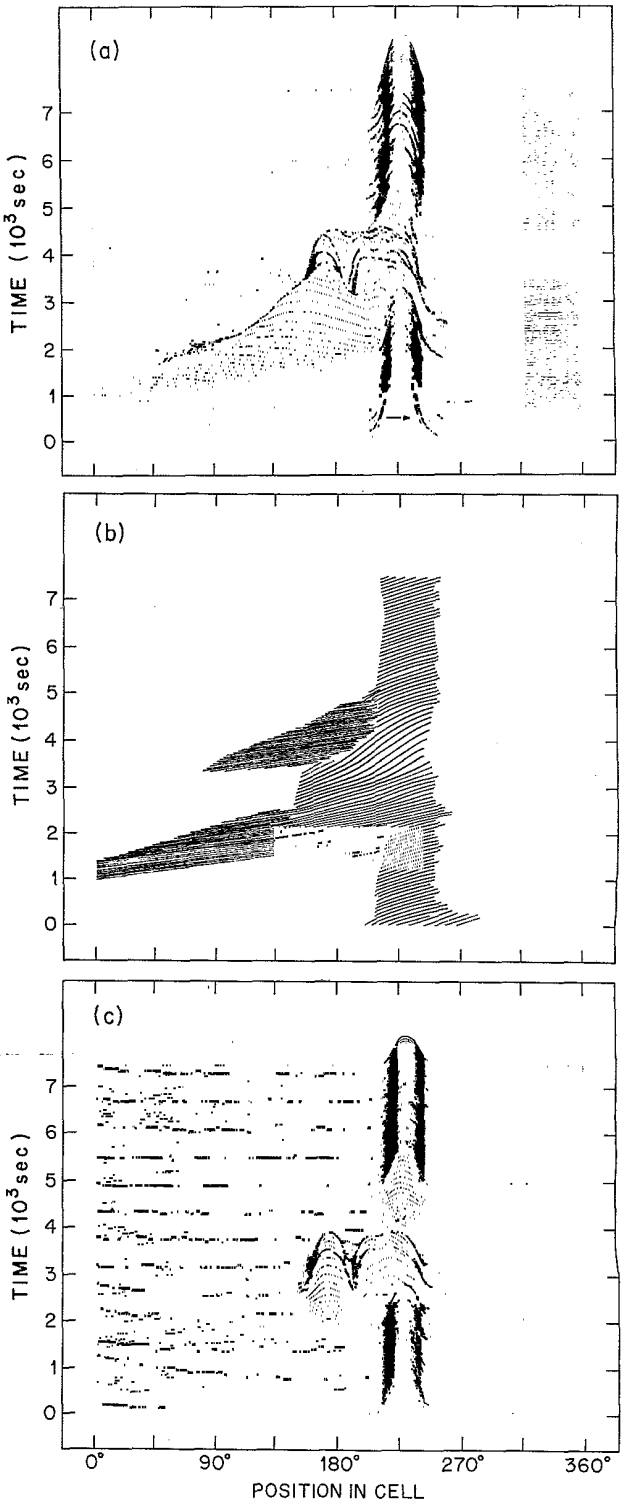

FIG. 17. Interaction between a pulse and a copropagating wave packet which grows into a pulse before collision, at $\epsilon=0.0062$. (a) Hidden-line plot of a wave packet growing up and interacting with a pulse to form a double-humped pulse. The double-humped pulse then decays back into a single-humped pulse. (b) Phase plot showing the coherent phase across the double-humped pulse. Note that the frequency shifts during the formation and destruction of the double-humped pulse. (c) Hidden-line plot showing the right-going low-frequency component of (a), calculated using frequency-sensitive complex demodulation.

higher phase velocity than the waves inside the pulses, creating phase dislocations at the boundary between the states. We do not display these phase dislocations here, because they appear in Fig. 5 of Ref. 4.

Our final category of experiments studied interactions between pulses. Since the pulses are stationary, they tend to drift together and interact only rarely and by chance. However, injected wave packets can create new pulses next to existing ones, and the resulting pair can interact. In Fig. 14, we show an injected right-going wave packet which grows up into a pulse next to an existing left-going pulse to create a counterpropagating pair. In Fig. 15(a), we show the subsequent evolution of this counterpropagating bound state. After a relatively long time, the right-going pulse annihilates the left-going pulse, leaving a single right-going pulse at the position of the original left-going pulse. The phase plot [Fig. 15(b)] shows the phase singularity at the intersection between the pulses and a left-going wave packet emitted at the time of the interaction.

In Fig. 16(a), we show the interaction of a pair of slowly drifting, copropagating, left-going pulses. The right pulse annihilates the left pulse and moves to the center of mass of the original pair. Because of the change in phase velocity across the pulse (mentioned above), there is a mismatch in phase at the boundary between the pulses [Fig. 16(b)] which creates phase defects. These defects propagate into the leading pulse, making it unstable. The phase of the surviving pulse is coherent with that of the trailing pulse that gave rise to it. The disappearing pulse also emits a wave packet, as in the counterpropagating case. It is not visible initially but grows as it circles the cell and collides with the surviving pulse.

In Fig. 17(a), we show another example in which an incident wave packet grows into a pulse next to a copropagating existing pulse. If we demodulate at the nonlinear frequency to isolate the right-going traveling waves [Fig. 17(c)], we see that the collision with the incident packet creates a double-humped nonlinear pulse comparable to Deissler and Brand's two-particle state.[12] After a short time, the double-humped pulse decays, and a single pulse reforms at the position of the original pulse. The demodulation also shows that the frequency of the stationary pulse shifts briefly away from its natural frequency both before the reassembling of the incident pulse and after its disappearance. The phase plot of the interaction shows that the incident wave packet resets the phase of the stationary pulse [Fig. 17(b)] and increases its frequency. When the double-humped pulse disappears, the frequency returns to normal, and a wave packet appears.

IV. DISCUSSION

We have observed three basic interactions between pulses and wave packets, depending on the amplitude of the wave packet. For small incident amplitudes, the pulse absorbs the wave packet completely without transmission or reflection. Similarly, below the threshold ϵ_f, pulses completely absorb the weak random fluctuations present in the cell, which therefore cannot grow into cell-filling rolls. Slightly larger wave packets reset the phase of the pulse and create weak transmitted waves, though no reflection occurs. The amplitude of the transmitted wave first increases and then decreases with the amplitude of the incident wave packet. Still larger packets destroy the pulse, often long after the collision. The destruction appears to be a consequence of the phase resetting which occurs during the collision. In the case of counterpropagating waves, the phase disturbances created by even the strongest incident wave packets propagate out of the pulse without destroying it.

The presence of fully absorbing pulses partially explains why the annulus is not immediately unstable to cell-filling convection above onset. For a range of positive ϵ, the quiescent state is convectively but not absolutely unstable to traveling-wave convention. A pulse, however, completely absorbs traveling waves generated by random fluctuations before they have time to grow into stationary pulses themselves. Only if the growth rate is large enough that these traveling waves can grow from the typical fluctuation amplitude to saturation over a length smaller than the separation between pulses can the cell-filling transition occur.

The reason that the pulses do not themselves spread to fill the cell for $\epsilon > 0$ must be sought in an extension of the existing Ginzburg-Landau theory.[7,9] The zero velocity of the pulses suggests that a single-field theory cannot provide a complete explanation. A possible extension is to add an additional field reflecting the vertical concentration gradient in the fluid and its nonlinear interaction with the convection amplitude.

We have also observed interactions between copropagating and counterpropagating pulses. In both cases, the pulses form a bound state. In the copropagating case, there are phase dislocations caused by the increase in phase velocity across the pulse. In the counterpropagating case, we find a grain boundary. In both cases, the bound state is unstable, with one pulse swallowing the other to leave a centered pulse which is phase coherent with one of the original pulses. Both events generate bursts of linear traveling waves.

These bound states of pulses and the destruction of one stable pulse by another are somewhat similar to effects seen in the model of Deissler and Brand.[12] However, they find that the fate of the colliding pulses depends primarily on pulse amplitude, with the larger pulse always surviving. We find instead that the pulse structure of the pulses is critical.[21] The pulses are a robust solution of the governing equations, with well-defined amplitudes and phase profiles. They can recover from small disruptions of phase caused by weak incident wave packets. However, larger phase disruptions make them unstable and lead o their disappearance, resulting in the emission of linear traveling waves. These effects are both seen clearly in Fig. 16(b), where the shift in phase velocity across the trailing pulse creates phase defects at the boundary with the copropagating leading pulse. These defects then propagate into the leading pulse, disturbing its phase structure and destroying it. However, the small phase disturbance caused by the collision with a wave packet [Fig. 7(b)] can be equally destructive. The long survival of the counterpropagating pulses seen in Fig. 15(b) results

from the inability of the phase defects of either pulse to propagate into the other, because they disturb the phase only at the leading edge. It would be useful to examine the case of counterpropagating pulses with the source of phase at their common boundary. Therefore, we must include phase structure, as well as non-Ginzburg-Landau effects, in any successful model of nonlinear pulses.

ACKNOWLEDGMENTS

We are pleased to acknowledge discussions with B. I. Shraiman, P. C. Hohenberg, W. van Saarloos, D. S. Cannell, G. Ahlers, H. R. Brand, and M. C. Cross, as well as technical assistance from H. Willliams.

[1]D. T. J. Hurle and E. Jakeman, J. Fluid Mech. **47**, 667 (1971).

[2]P. Kolodner, J. A. Glazier, and H. Williams, Phys. Rev. Lett. **65**, 1579 (1990); J. A. Glazier, P. Kolodner, and H. Williams, J. Stat. Phys. (to be published).

[3]J. J. Niemela, G. Ahlers, and D. S. Cannell, Phys. Rev. Lett. **64**, 1365 (1990).

[4]K. E. Anderson and R. P. Behringer, Phys. Lett. A **145**, 323 (1990).

[5]P. Kolodner and J. A. Glazier, Phys. Rev. A **42**, 7504 (1990).

[6]D. R. Ohlsen, S. Y. Yamamoto, C. M. Surko, and P. Koldner, Phys. Rev. Lett. **65**, 1431 (1990); P. Kolodner and J. A. Glazier (unpublished).

[7]W. van Saarloos and P. C. Hohenberg, Phys. Rev. Lett. **64**, 749 (1990).

[8]E. Moses, J. Fineberg, and V. Steinberg, Phys. Rev. A **35**, 2757 (1987); R. Heinrichs, G. Ahlers, and D. S. Cannell, *ibid.* **35**, 2761 (1987).

[9]O. Thual and S. Fauve, J. Phys. (Paris) **49**, 1829 (1988).

[10]S. Fauve and O. Thual, Phys. Rev. Lett. **64**, 282 (1990).

[11]V. Hakim, P. Jakobsen, and Y. Pomeau, Europhys. Lett. **11**, 19 (1990); C. Elphick and E. Meron, Phys. Rev. A **40**, 3226 (1989); B. A. Malomed and A. A. Nepomnyashchy (unpublished).

[12]R. J. Deissler and H. R. Brand, Phys. Lett. A **130**, 293 (1988); H. R. Brand and R. J. Deissler, Phys. Rev. Lett. **63**, 2801 (1989); R. J. Deissler and H. L. Brand, Phys. Lett. A **146**, 252 (1990).

[13]W. Barten, M. Lücke, and M. Kamps (unpublished).

[14]P. Kolodner, H. Williams, and C. Moe, J. Chem. Phys. **88**, 6512 (1988).

[15]P. Kolodner and H. Williams in *Proceedings of the NATO Advanced Research Workshop on Nonlinear Evolution of Spatio-temporal Structures in Dissipative Continuous Systems,* Vol. 225 of NATO Advanced Study Institute, Series B2, edited by F. H. Busse and L. Kramer (Plenum, New York, 1990), p. 73.

[16]M. C. Cross and K. Kim, Phys. Rev. A **37**, 3909 (1988).

[17]P. Kolodner, C. M. Surko, A. Passner, and H. L. Williams, Phys. Rev. A **36**, 2499 (1987).

[18]P. Kolodner, A. Passner, C. M. Surko, and R. W. Walden, Phys. Rev. Lett. **56**, 2621 (1986); C. M. Surko and P. R. Kolodner, *ibid.* **58**, 2055 (1987).

[19]D. S. Cannell and G. Ahlers have also observed such fluctuations (private communication). I. Rehberg, S. Rasenat, M. de la Torre, W. Schöpf, F. Hörner, G. Ahlers, and H. R. Brand (unpublished) have studied spontaneous traveling-wave fluctuations and their divergent amplification near the onset of electrohydrodynamic convection. W. Schöpf and I. Rehberg (unpublished) have performed similar studies in convection in a binary fluid in a narrow channel.

[20]P. Kolodner, C. M. Surko, and M. C. Cross (unpublished).

[21]R. J. Deissner and H. R. Brand have examined phase structure theoretically (unpublished).